Quantitative Four-State Conformational Analysis by Ring Current NMR Anisotropy: A Family of Molecules Capable of Intramolecular π-Stacking

Jing Chen[a] and Arthur Cammers-Goodwin*[a]

Dedicated to Robert D. Guthrie, Professor of Physical Organic Chemistry, on the occasion of his retirement after 37 years of service

Keywords: Conformation analysis / NMR spectroscopy / Molecular dynamics / Density functional calculations / Stacking interactions

A novel, multi-state, conformational analysis based on the magnetic anisotropy of molecules undergoing fast dynamic exchange is described. Calculated chemical shift tensors combined with experimental data from proton NMR studies were used to quantify conformational distributions as a function of solvent and temperature for a hydrocarbon and two fluorocarbon derivatives of *N*,*N*′-[1,3-phenylenebis(methylene)]bis(2-phenylpyridinium) dibromide. Inspection for adequate analyses involved confirming that the mathematical expressions conserved magnetization (mass). Enthalpic parameters from VT-NMR gave some indication of the nature of the impact of solvent on conformation. Results indicated that electrostatic interactions between aromatic rings can strongly impact organic conformation in solution.

Introduction

Conformational isomerism is a key issue in the study of biological molecules and is potentially useful in the development of drugs. More than any other spectroscopic technique, NMR methods have aided the study of conformation of organic and biological molecules. These methods most often give unambiguous answers when the molecule under study possesses one stable conformer (native state) or possesses two or three conformers that exchange slowly compared to the NMR time scale. In both cases, analysis of NMR coupling constants, NOE, and integration can be incisive.[1] However, quantitative conformational distributions are difficult to determine when multiple conformers interconvert rapidly.

Using time-averaged coupling and chemical shift data to quantify dynamic rotamer populations has tantalized chemists for the past 40 years.[2] For appropriate structures, analysis of conformationally diagnostic coupling constants can lead to quantitative, multi-state, conformational distributions.[3−6] However, coupling and the influence of diamagnetic anisotropy of aromatic groups[7] on chemical shifts are usually used to qualitatively investigate conformation.[8−18] In a study related to the current work, ab initio chemical shift calculations have identified the most probable single conformer of [10]annulene.[19,20] Also pertinent to this work is a three-state conformational distribution reported for a cyclophane using ^{19}F, ^{13}C and ^{1}H NMR spectrometry.[21]

Derivatives of molecules **1**−**3** are interesting because they have served as models for intramolecular π-stacking.[22−24] In this study compound **4** served as the NMR chemical shift reference for calculations and experiments. Compounds **1** and **4** were used in recent work in which ab initio calculations of chemical shifts were used for the first time with modeling and NMR experiments in order to quantify multi-conformer, dynamic equilibria.[25,26] The results of the current study put some of the conclusions of the previous work in question. These incongruities are summarized and discussed in the conclusion section. In the current study, the inclusion of compounds **2** and **3** with a novel computational shortcut made it possible to balance the total magnetism and to define four states in temperature and solvent-dependent, dynamic equilibria. These two achievements, reported here for the first time, highlight the novelty of this work.

Results and Discussion

The current analysis started with the premise that dividing structures **1**−**3** along the C_2 axis that passes through H_a and H_c (Figure 1) and considering only states defined by two rings simplified the mathematics and allowed extrapolation to the dynamic behavior of the real molecules.

[a] Chemistry Department, University of Kentucky, Chemistry/Physics,
Lexington KY, USA
Fax: (internat.) +1-859-323-1069
E-mail: a.cammers@uky.edu

 DOI: 10.1002/ejoc.200300302

Monte Carlo conformational searching of **1** using the AMBER* force field and the GB/SA $CHCl_3$ solvent model as implemented by MacroModel 8.1[27,28] produced a collection of conformers that were grouped into macrostates **C** (cluster), **F** (face-to-face) and **S** (splayed) shown in Figure 2. Conformers **C** and **F** are considered "stacked" whereas **S** dissociated the all-carbon aromatic rings. The two-ring analysis allowed mixed three-ring states like **CF** and **CS**, etc. on the same or on opposite sides of the xylyl moiety.

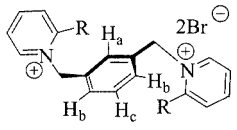

1–4

Figure 1. **1**: R = phenyl, **2**: R = 2,4,6-trifluorophenyl; **3**: R = pentafluorophenyl; **4**: R = methyl

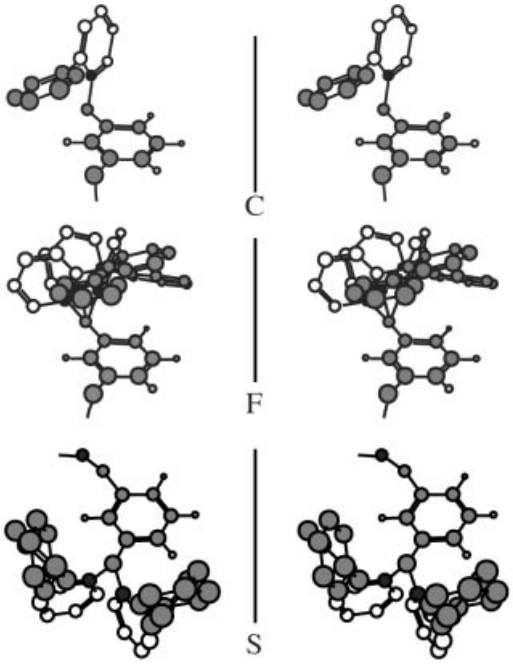

Figure 2. Stereoviews of the two-ring microstates used to compose the **C, F** and **S** states

A single conformer, in which the phenyl ring occupied space in front of H_a, modeled the xylyl chemical shifts in molecules **1**−**3** of the **C** state. When both phenyl groups adopted **C** state conformation, the two phenyls and the xylyl moieties made contact. In **C** the upfield anisotropic contribution to the chemical shift at H_a was much greater than H_b. NMR chemical shift calculations of three conformational microstates were used to model the chemical shifts of the **F** state. In two of these, the phenyl centroids in **1**−**3** were proximal to H_a and H_b, respectively. **F** also included a microstate which placed the phenyl group in front of H_b in a manner analogous to the position of the phenyl group with respect to H_a in conformer **C**. Unlike conformer **C**, the two phenyl rings in this microstate could not make contact. Molecular modeling indicated minimal energetic differences between these three microstates. A dynamic average with equal weighting of these three states comprised the **F** state.

Modeling the chemical shifts of the **S** state required four microstates because four low-energy conformers, unrelated by symmetry, dissociated the aromatic rings. Two shallow energy wells from the rotation of the xylyl-CH_2 bond divided the **S** state into two conformers (**5S** and **6S**). These two states were further divided into four conformational microstates associated with the biphenyl torsional angle (**5See**−**6Sef** in Figure 3). In the **See** states the edges of phenyl and xylyl met and in the **Sef** states phenyl faced the edge of xylyl. **See** and **Sef** states were not expected to be isoenergetic.[29]

The microstates of **S** of **1, 2** and **3** were similar, but not identical. When the hydrogen atoms on the phenyl ring were substituted with fluorine atoms, H_a and H_b occupied space within the van der Waals radius of one *ortho* fluorine atom of molecules **2** and **3** in microstates **5See** and **6See** respectively. Small changes in the biphenyl dihedral angle by modeling local minima removed these steric interactions.

Calculation of Conformational Distributions

Equations (1)−(4) were used to solve for the mol fractions of **C, F** and **S.** Equation (1) expresses mass balance and Equations (2)−(4) describe the differences in the chemical shifts of H_a, H_b and H_c between molecules **1**−**3** versus reference molecule **4** as a function of conformational distribution. X_{Cm} in Equation (2) is the mol fraction of one phenyl and a xylyl ring in the **C** conformation in molecule m (m = 1, 2 or 3) and C_{am} is the magnetic contribution of conformer **C** to the difference in the chemical shifts of H_a in molecule m versus reference molecule **4**. Terms in Equations (2)−(4) have analogous meanings.

$$X_{\mathbf{C}m} + X_{\mathbf{F}m} + X_{\mathbf{S}m} = 1 \quad (1)$$

$$\delta_{4\mathrm{Ha}} - \delta_{m\mathrm{Ha}} = 2C_{am}X_{\mathbf{C}m} + 2F_{am}X_{\mathbf{F}m} + 2See_{am}X_{\mathbf{See}m} + 2Sef_{am}X_{\mathbf{Sef}m} \quad (2)$$

$$\delta_{4\mathrm{Hb}} - \delta_{m\mathrm{Hb}} = C_{bm}X_{\mathbf{C}m} + F_{bm}X_{\mathbf{F}m} + See_{bm}X_{\mathbf{See}m} + Sef_{bm}X_{\mathbf{Sef}m} \quad (3)$$

$$\delta_{4\mathrm{Hc}} - \delta_{m\mathrm{Hc}} = 2C_{cm}X_{\mathbf{C}m} + 2F_{cm}X_{\mathbf{F}m} + 2See_{cm}X_{\mathbf{See}m} + 2Sef_{cm}X_{\mathbf{Sef}m} \quad (4)$$

Calculations of the constants C_{am}, F_{am}, See_{am}, Sef_{am}, and the corresponding constants for H_b, and H_c that appear in Table 1 were performed with Gaussian98™ using rb3lyp/6−311++g(2d,2p), and keyword NMR.[30] Because accurate calculations demanded a lot of CPU time, structural abbreviations shown in Figure 4 were made to perform minimalist closed-shell calculations. For each component conformational microstate used in the construction of **C, F** and **S,** the effects of magnetic anisotropy of the phenyl rings on the xylyl chemical shifts were computed by deleting all

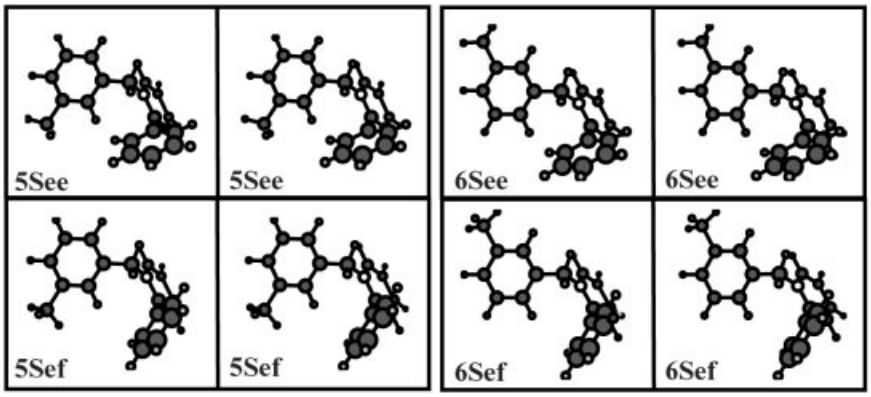

Figure 3. Stereoviews of the four microstates used to compose the **S** state

rings except two and substituting the pyridinium group with fluorine atom, **7** in Figure 4. The fluorine atom is the minimalist, electronegative, heavy atom with a closed shell. Unsubstituted sp^2 carbon atoms in the xylyl ring were replaced with hydrogen atoms; the other xylyl carbon atoms were deleted, **8** in Figure 4. After these operations were complete, the relative positions of the original atoms were not changed. The calculated shielding of H_a in **9** minus the same in **8** (in the spatial arrangement corresponding to the **C** state) was used as C_{a1}. Similar calculations with **10** (X = H and F) gave values for C_{a2} and C_{a3}. Performing these minimalist calculations gave results similar to results from more complex calculations of molecule **1** in a fraction of the time.[25] Coefficients F_{am} and S_{am} were averages of the coefficients of their constituent microstates, and these were calculated similarly to C_{a1}.

Table 1. Equations used to translate changes in chemical shift to mol fractions of C, F and S of molecules **1**−**3**

	C	F	See	Sef
a1	1.70	0.52	−1.61	0.14
b1	0.19	1.26	−0.67	0.22
c1	0.07	0.40	0.27	0.25 (0)[a]
a2	1.49	0.39	−0.55	0.16
b2	0.11	1.03	−0.17	0.20
c2	0.05	0.25	0.10	0.17 (0)[a]
a3	1.52	0.36	−0.97	0.20
b3	0.07	0.97	−0.39	0.21
c3	0.03	0.30	0.09	0.20 (0)[a]

The calculations of the coefficients for the chemical shifts of H_b [Equation (3)] were more complicated than those of H_a and H_c. Note that Equations (2) and (4) are multiplied by two whereas Equation (3) is not. Magnetic anisotropy from the two phenyl groups operated identically on H_a and H_c in molecules **1**−**3**, hence the factor two. However, H_b and H_b' (**8**) shared the magnetic effect of the two phenyl groups. Furthermore the shielding effects on H_b and H_b' by one phenyl group were different. Coefficients C_{bm}, F_{bm} and S_{bm} for m = **1**−**3** were sums of these two different magnetic effects.

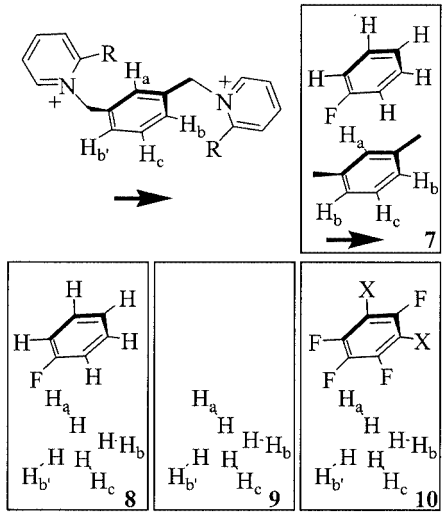

Figure 4. Steps taken to simplify the structures for chemical shift calculations

A major caveat when setting up NMR calculation-based conformational analyses concerns the way anisotropy must be averaged. Structures cannot be averaged to perform fewer calculations of the chemical shifts. The chemical shifts of microstates need to be calculated and then these values need to be averaged to create constants for equations like 2, 3 and 4. In general, the chemical shifts calculated for an averaged structure of multiple conformational microstates is not necessarily the average chemical shift of the conformational microstates.

The gas-phase chemical shift calculations overestimated the solution-phase upfield shift due to ring current when conformations held the observed proton greater than 6 Å from the ring in intense regions of the shielding cone. At distances beyond 6 Å the effects of diamagnetic ring current are negligible.[31,32] At these distances, solvent molecules shield the observed protons from local magnetic anisotropy. H_c in **Sef** occupied a highly shielded region, but too far from phenyl to produce an appreciable ring current effect. Thus, in the expression for δH_c [Equation (4), Table 1] the over-estimated coefficients for the **Sef** state were assumed

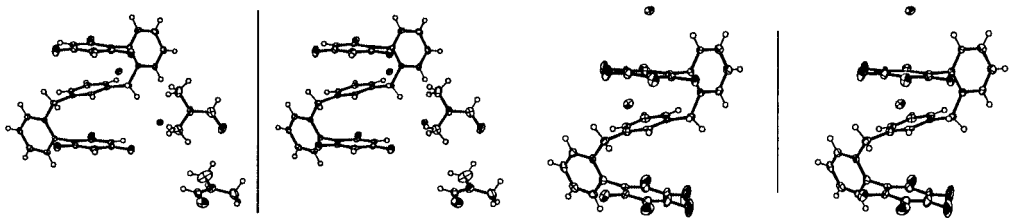

Figure 5. Stereoviews: solid states of **1** (not shown), **2** (left), and **3** (right) were **F**-like

to be zero. These corrections turned negative mol fractions into positive mol fractions of conformers in graphs 6.1−6.3.

Physical Studies

Molecules **1**−**3** were expected to share similar conformational space because substituents on the edges of the rings should not have hindered interactions between aromatic groups in conformers **C** and **F** of **1**−**3**. Furthermore the often quoted isosteric relationship between fluorine and hydrogen atoms meant minimal structural perturbation upon substitution.[33−35]

There was an obvious preference for **F**-like solid states given that **1** crystallized with two water molecules,[25] **2** crystallized with two molecules of DMF and **3** crystallized with only **3** and bromide in the lattice. Intramolecular π-stacking in the solid states of related structures appears to be the rule instead of the exception.[24,36]

Small increments in the distance between the xylyl and phenyl centroids in the series **1**, **2** and **3** (3.94, 3.95, and 4.23 Å, respectively) in the solid states may have indicated increasing coulombic repulsion between the aromatic rings. The quadruple moments of benzene and hexafluorobenzene are approximately the same magnitude but differ in sign.[37] Putative electrostatic character in aromatic structures have united many themes in solution and solid state studies of cation-π and aromatic interactions.[38−44]

Conformational analysis should be sound under a variety of conditions. [D_6]DMSO is an attractive aqueous NMR co-solvent to perturb the conformational distribution because it has broad application to the chemical and biological sciences.[45,46] Figure 6 depicts the results from a series of NMR titrations done by adding DMSO to separate samples of molecules **1**−**4** in D_2O. The data in Figure 6 were processed by finding simultaneous solutions of Equations (1)−(4) with experimental values of $\delta_4-\delta_m$ for H_a, H_b, and H_c.

Electrostatic interactions between the aromatic rings apparently contributed to the solution state conformations of **1**−**3** because the fluorinated phenyls in **2** and **3** associated less with the xylyl ring than the phenyl in **1**. Electrostatic effects on the solution states of similar molecules has been reported recently.[22] Figure 6 shows that the sum of **S** state mol fractions increased with the number of fluorine atoms on the phenyl rings. Geometrical dependencies of aromatic electrostatic interactions were apparently also reflected in the conformations of **1**−**3**. The left graph in Figure 6 shows that **1** preferentially adopted conformer **Sef** with xylyl and phenyl positioned edge-to-face whereas **2** and **3** preferred **See** with xylyl and phenyl positioned edge-to-edge. The relative populations of C, F, X_{See}, and X_{Sef} for **1**−**3** were different, but they all were perturbed in the same direction upon titration with DMSO, a good indication that these

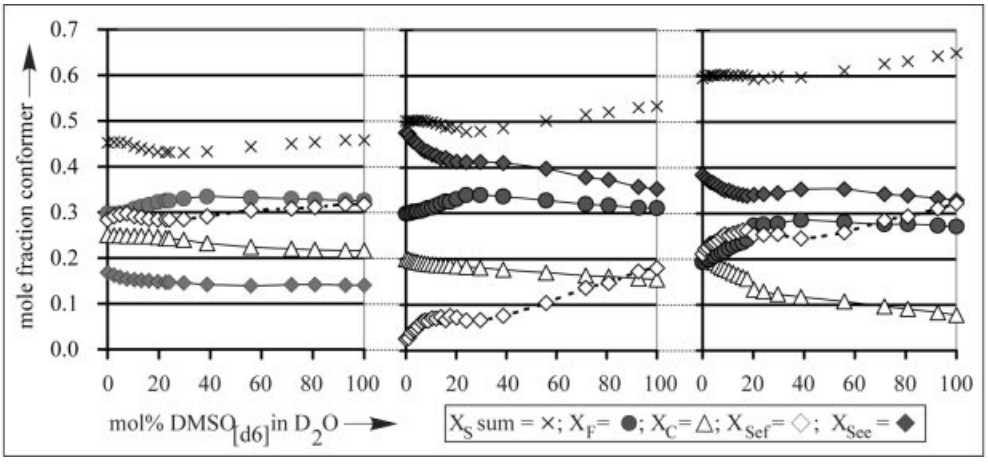

Figure 6. Graphs of the mol fractions of conformers **C, F**, and **S** as a function of the mol % DMSO in D_2O for compounds **1**−**3**. From left to right: four-state solutions of Equations (1)−(4) for compounds **1**−**3**, respectively. The precision of the graphs is within the size of the icons and is discussed further in the footnote of Table 2. The accuracy of the graphs (within 10%) depended on the accuracy of the chemical shift calculations[30] and on how well the modeling-derived microstates represented the total distributions of conformers.

labels had similar structural significance in all three molecules.

The reader will note that the expression for mass balance in the system of four equations in Table 1 stipulated that the mol fractions in the solution of the four simultaneous equations sum to unity. This system of equations allowed negative mol fractions. The fact that the mol fractions were positive under different solvent conditions and temperature served as an internal check of the coefficients in Table 1. The coefficients were checked again in the following manner. Solving a system of equations for the mol fractions of **C** and **F** and an averaged **S** state, unbound by mass, using only expressions for chemical shifts like those in Equations (2)−(4) produced mol fractions that summed to 1.0 ±0.2 over the course of the DMSO titrations. This result meant that the differences in magnetization between **4** and **1**−**3** were probably adequately reflected by the coefficients and that the subset of conformations used to describe the conformational distributions of **1**−**3** were probably sufficient.

The enthalpies from van't Hoff analysis of the conformational distribution ($\ln[K_{c1}] = -\Delta H/RT + \Delta S/R$; $K_{c1} = X_{c1}/[1 - X_{c1}]$) in pure D_2O and DMSO in Table 2 reflected the stabilities that one might have predicted from the three graphs in Figure 6. The aqueous **C** state and DMSO **F** state appeared to possess native stability. The signs of these enthalpies readily switched under the influence of solvent in directions one would not a priori have predicted if the electrostatic nature of the rings controlled conformation. The **C** and **F** states associated aromatic rings with complementary electrostatic interactions in molecules **1**−**3**; however, transfer from aqueous to organic media brought about opposite changes in the stabilities of the two states for molecules **1**−**3**.

Table 2. Enthalpies in kcal/mol from van't Hoff analysis

Molecule (solvent)	ΔH_C	ΔH_F	ΔH_{See}	ΔH_{Sef}
1 (D_2O)	−0.68	0.60	−0.17	0.11
1 (DMSO)	−0.17	−0.62	0.25	0.60
2 (D_2O)	−0.82	0.56	−0.37	[a]
2 (DMSO)	0.17	−0.75	0.26	0.66
3 (D_2O)	−1.20	0.92	−0.40	0.83
3 (DMSO)	0.34	−0.98	0.26	0.51

Because solvent molecules could not occupy space between the aromatic moieties in **1**−**3**, the solvent effect on conformation must have involved changing external dielectric and a more or less constant internal dielectric. The relative tendency to dissociate face-to-face rings in **1**−**3** (total **S** state mol fraction in graphs 6.1−6.3) probably involved aromatic/ aromatic electrostatic interactions in the context of low internal dielectric constants. Energies from molecular modeling calculations designed to mimic the effect of solvent agreed roughly with the NMR conformational analysis. The **F** state was favored over the **C** state in organic solvent whereas the situation was reversed in water (AMBER* and the MM2* force field using GB/SA water, $CHCl_3$). Accounting for microscopic dielectric as a function of excluded solvent volume was the major problem that the development of the GB/SA solvent model sought to solve.[27] The fact that changes in a calculated external dielectric in the GB/SA solvent model roughly predicted conformational changes indicated that solvent-dependent, surface electrostatic interactions played a major role in shifting conformational populations in these dications.

Conclusion

Previous conformational analysis of **1** generated the hypothesis that dispersive interactions at the aromatic edges between solvent and **1** favored the **F** state because shifts in conformer population did not rigorously scale with bulk dielectric constant, and depended heavily on the degree of solvent fluorination.[26] Fluorinating the conformational solvent probe in this work rigorously tested the level of involvement of these dispersive interactions. Graphs 6.1−6.3 show that fluorination did not change the solvent-dependence of the conformers, thus edge-wise dispersive interactions could not be responsible for the solvent effect on conformation in **1**−**3**. Increasing the mol % DMSO stabilized the **F** state and destabilized the **C** state for **1**−**3**. If dispersive interactions between solvent and **1**−**3** were important, trends in the conformational solvent dependence of **1** versus **2** and **3** would have differed.

This work suggests a general protocol for the application of ring current to quantitative conformational analysis. Using a consistent method of conformational analysis with **1**−**3** required more sophistication than the analysis of **1** alone.[25] Quantitatively determining multiple conformers with ring current depended greatly on a good internal reference and the meticulous inclusion of conformational microstates in the distribution. When all the microstates described above were not included, negative mol fractions for **2** and **3** were obtained. While new details came to light with inclusion of **2** and **3** in the conformational analysis, the general trends in the solvent-dependent conformational distribution of **1** in the previous analysis were corroborated.[25]

Experimental Section

General Remarks: All ^1H NMR experiments were performed at 400 MHz using two NMR tubes; one tube contained **1**, **2**, or **3** and the other contained reference compound **4** in an identical solvent matrix. Measurements were performed under strict control of temperature. After any change in solvent or temperature, the chemical shifts were monitored until they remained constant, indicating thermal equilibrium. The chemical shifts were recorded to three digits past the decimal. The NMR probe thermometer was corrected with the MeOH chemical shift-based temperature scale. For characterization, slight magnetic inequivalences in **2** and **3** are reported below as pseudo first order splitting patterns. All ^{19}F NMR spectra were referenced to $CFCl_3$.

X-ray diffraction data were collected at 90 K with a Nonius−Kappa CCD diffractometer from crystals mounted in pa-

ratone oil. Raw data were integrated, scaled, merged and corrected for Lorentz-polarization effects by using the HKL-SMN package.[47] The structure was solved by direct methods (SHELXS-97) and difference Fourier (SHELXL-97). Refinement was carried out against F2 by weighted full-matrix least-squares (SHELXL-97). Hydrogen atoms were found in difference maps and subsequently placed at calculated positions and refined using riding models with isotropic displacement parameters derived from their attached atoms. Non-hydrogen atoms were refined with anisotropic displacement parameters. Atomic scattering factors were taken from the International Tables for Crystallography.[48]

CCDC-196724 and -196725 contain supplementary crystallographic data for compounds **2** and **3**, respectively. These data can be obtained free of charge at www.ccdc.cam.ac.uk/conts/retrieving.html [or from the Cambridge Crystallographic Data Centre, 12, Union Road, Cambridge CB2 1EZ, UK; fax: (internat.) +44-1223-336-033; E-mail: deposit@ccdc.cam.ac.uk].

Raw chemical shift data was recorded in a spreadsheet and linear algebra[49] was performed on the data to obtain the mol fractions of conformers from Equations (1)−(4).

Trifluorophenyl Dication 2: α,α′-*m*-Xylyl dibromide (89.7 mg, 0.34 mmol) and 2-(2,4,6-trifluorophenyl)pyridine,[50] (142.1 mg, 0.68 mmol) were dissolved in dry DMF (0.3 mL) in a flask fitted with a stir bar and an airtight stopper. The solution was heated in an oil bath at 70−80 °C for 12 h. After evaporation of DMF, the solid residue was triturated three times with a mixture of diethyl ether and 2-propanol (1:3) to obtain a white solid pure by ^{1}H NMR (86%); m.p. 184−186 °C. ^{1}H NMR (400 MHz, D_2O): δ = 9.19 (dd, $J_{H,H}$ = 6.4, 1.2 Hz, 2 H, pyridinium C6-H), 8.75 (ddd, $J_{H,H}$ = 8.0, 8.0, 1.5 Hz, 2 H, pyridinium C4-H), 8.27 (ddd, $J_{H,H}$ = 8.0, 6.4, 1.5 Hz, 2 H, pyridinium C5-H), 8.17 (dd, $J_{H,H}$ = 8.0, 1.5 Hz, 2 H, pyridinium C3-H), 7.27 (t, $J_{H,H}$ = 8.0 Hz, 1 H, xylyl H_c), 7.01 (t, $J_{H,F}$ = 8.9 Hz, 4 H, trifluorophenyl C−H), 6.99 (d, $J_{H,H}$ = 8.0 Hz, 2 H, xylyl H_b), 6.50 (s, 1 H, xylyl H_a), 5.71 (s, 4 H, methylene) ppm. ^{13}C NMR (100 MHz, D_2O): δ = 165.5 (dt, $J_{C,F}$ = 251, 15.2 Hz, *para*-C−F), 159.6 (ddd, $J_{C,F}$ = 252, 15.5, 7.8 Hz, *ortho*-C−F), 147.9, 147.4, 143.7, 133.7, 133.3, 130.3, 129.2, 129.0, 125.8, 105.4 (td, $J_{C,F}$ = 20.0, ≈3.9 Hz, trifluorophenyl quaternary C), 101.8 (ddd, $J_{C,F}$ = 25.8, 25.8, 3.5 Hz, trifluorophenyl *m*-C-H), 62.7 ppm. ^{19}F NMR (377 MHz, D_2O): δ = 167.2 (≈p, tt, $J_{F,H}$ = 8.9, J_{FF} = 9.0 Hz, 1 F), 159.3 (dd, $J_{F,H}$ = 8.9, J_{FF} = 9.0 Hz, 2 F) ppm. MS/MS: *m*/*z* = 705 $[M + Na]^+$, 602 $[M + Br]^+$, 261 $[M - 2Br]^{2+}$. X-ray diffraction analysis of the solid crystallized from DMF confirmed connectivity.

Pentafluorophenyl Dication 3: Procedure was analogous to the one above except 2-(pentafluorophenyl)pyridine,[50] was used as the nucleophile. Yield 77%, m.p. 188−190 °C. ^{1}H NMR (400 MHz, D_2O): δ = 9.30 (dd, $J_{H,H}$ = 6.4, 1.0 Hz, 2 H, pyridinium C6-H), 8.87 (ddd, $J_{H,H}$ = 8.0, 8.0, 1.3 Hz, 2 H, pyridinium C4-H), 8.40 (ddd, $J_{H,H}$ = 8.0, 6.4, 1.5 Hz, 2 H, pyridinium C5-H), 8.30 (dd, $J_{H,H}$ = 8.0, 1.2 Hz, 2 H, pyridinium C3-H), 7.40 (t, $J_{H,H}$ = 7.8 Hz, 1 H, xylyl H_c), 7.20 (dd, $J_{H,H}$ = 7.8, 1.5 Hz, 2 H, xylyl H_b), 6.70 (s, 1 H, xylyl H_a), 5.80 (s, 4 H, methylene) ppm. ^{13}C NMR (100 MHz, D_2O): δ = 148.5, 147.9, 144.0 (dm, $J_{C,F}$ = 252 Hz, *ortho*-C−F), 141.0, 138.2 (dm, $J_{C,F}$ = 256 Hz, *meta*-C−F), 133.7, 133.4, 130.5, 130.1, 129.5, 126.0, 117.4 (dm, $J_{C,F}$ = 333 Hz, *para*-C−F), 105.7(m), 62.6 ppm. ^{19}F NMR (377 MHz, D_2O): δ = 128.0 (d, J_{FF} ≈18.5 Hz, 2 F), 119.6 (t-like, J_{FF} ≈21.0 Hz, 1 F), 106.9 (dd, J_{FF} ≈21.0, J_{FF} ≈18.5 Hz, 2 F) ppm. MS/MS: *m*/*z* = 777 $[M + Na]^+$, 674 $[M^2 + Br]^+$, 297 $[M - 2Br]^{2+}$. X-ray diffraction analysis of the solid crystallized from DMF confirmed connectivity.

Acknowledgments

The authors thank the National Science Foundation USA #0111578 for funding this research.

[1] P. M. Marcos, J. R. Ascenso, J. L. C. Pereira, *Eur. J. Org. Chem.* **2002**, 3034−3041.
[2] G. J. Karabatsos, D. J. Fenoglio, in *Topics in Stereochemistry*, vol. 5 (Eds.: E. L. Eliel, N. L. Allinger), Wiley Interscience, New York, **1970**, pp. 167.
[3] P. Cimino, G. Bifulco, A. Evidente, M. Abouzeid, R. Riccio, L. Gomez-Paloma, *Org. Lett.* **2002**, *4*, 2779−2782.
[4] D. R. Kent, IV, N. Dey, F. Davidson, F. Gregoire, K. A. Petterson, W. A. Goddard, III, J. D. Roberts, *J. Am. Chem. Soc.* **2002**, *124*, 9318−9322.
[5] S. Kurtkaya, V. Barone, J. E. Peralta, R. H. Contreras, J. P. Snyder, *J. Am. Chem. Soc.* **2002**, *124*, 9702−9703.
[6] A. M. Belostotskii, M. Shokhen, H. E. Gottlieb, A. Hassner, *Chem. Eur. J.* **2001**, *7*, 4715−4722.
[7] C. W. Haigh, R. B. Mallion, *Progress in N. M. R. Spectroscopy* **1979**, *13*, 303−344.
[8] A. M. Belostotskii, H. E. Gottlieb, P. Aped, *Chem. Eur. J.* **2002**, *8*, 3016−3026.
[9] V. Berl, I. Huc, R. G. Khoury, J.-M. Lehn, *Chem. Eur. J.* **2001**, *7*, 2798−2809.
[10] Y. Fukazawa, S. Usui, K. Tanimoto, Y. Hirai, *J. Am. Chem. Soc.* **1994**, *116*, 8169−8175.
[11] Y. Fukazawa, T. Hayashibara, Y. Y. Yang, S. Usui, *Tetrahedron. Lett.* **1995**, *36*, 3349−3352.
[12] Y. Fukazawa, Y. Y. Yang, T. Hayashibara, S. J. Usui, *Tetrahedron* **1996**, *52*, 2847−2862.
[13] Y. Shigemitsu, M. Juro, Y. Mukuno, Y. Odaira, *Bull. Chem. Soc. Jpn.* **1978**, *51*, 1249−1250.
[14] H. Iwamoto, Y. Y. Yang, S. Usui, Y. Fukazawa, *Tetrahedron Lett.* **2001**, *42*, 49−51.
[15] T. Bürgi, A. Baiker, *J. Am. Chem. Soc.* **1998**, *120*, 12920−12926.
[16] S. H. Gellman, T. S. Haque, L. F. Newcomb, *Biophys. J.* **1996**, *71*, 3523−3525.
[17] G. Moyna, R. J. Zauhar, H. J. Williams, R. J. Nachman, A. I. Scott, *J. Chem. Inf. Comput. Sci.* **1998**, *38*, 702−709.
[18] M. Lofthagen, J. S. Siegel, *J. Org. Chem.* **1995**, *60*, 2885−2890.
[19] D. R. Price, J. F. Stanton, *Org. Lett.* **2002**, *4*, 2809−2811.
[20] T. Sternfeld, R. E. Hoffman, M. Saunders, R. J. Cross, M. S. Syamala, M. Rabinovitz, *J. Am. Chem. Soc.* **2002**, *124*, 8786−8787.
[21] H. Takemura, H. Kariyazono, N. Kon, T. Shinmyozu, T. Inazu, *J. Org. Chem.* **1999**, *64*, 9077−9079.
[22] M. J. Rashkin, M. L. Waters, *J. Am. Chem. Soc.* **2002**, *124*, 1860−1861.
[23] C. B. Martin, H. R. Mulla, P. G. Willis, A. Cammers-Goodwin, *J. Org. Chem.* **1999**, *64*, 7802−7806.
[24] C. B. Martin, B. O. Patrick, A. Cammers-Goodwin, *J. Org. Chem.* **1999**, *64*, 7807−7812.
[25] H. R. Mulla, A. Cammers-Goodwin, *J. Am. Chem. Soc.* **2000**, *122*, 738−739.
[26] M. D. Sindkhedkar, H. R. Mulla, A. Cammers-Goodwin, *J. Am. Chem. Soc.* **2000**, *122*, 9271−9277.
[27] F. Mohamadi, N. G. J. Richards, W. C. Guida, R. Liskamp, M. Lipton, C. Caufield, G. Chang, T. Hendrickson, W. C. Still, *J. Comp. Chem.* **1990**, *11*, 440−467.
[28] M. Scarsi, J. Apostolakis, A. Caflisch, *J. Phys. Chem. B.* **1998**, *102*, 3637−3641.
[29] For a comprehensive discussion of edge-to-face π-stacking interactions, see: W. B. Jennings, B. M. Farrell, J. F. Malone, *Acc. Chem. Res.* **2001**, *34*, 885−894.
[30] For a discussion of the accuracy of NMR chemical shifts as a function of computational method, see: J. R. Cheeseman, G. W. Trucks, T. A. Keith, M. J. Frisch, *J. Chem. Phys.* **1996**, *104*, 5497−5509.

[31] Y. Fukazawa, K. Ogata, S. Usui, *J. Am. Chem. Soc.* **1988**, *110*, 8692−8693.

[32] M. P. Williamson, T. Asakura, *J. Magn. Reson.* **1991**, *94*, 557−562.

[33] G. A. Patani, E. J. LaVoie, *Chem. Rev.* **1996**, *96*, 3147−3176.

[34] Y. Takeuchi, T. Shiragami, K. Kimura, E. Suzuki, N. Shibata, *Org. Lett.* **1999**, *1*, 1571−1573.

[35] C. W. Thornber, *Chem. Soc. Rev.* **1979**, *8*, 563−580.

[36] D. R. Body, T. A. Evans, W. B. Jennings, J. F. Malone, W. OSullivan, A. Smith, *Chem. Commun.* **1996**, 2269−2270.

[37] J. H. Williams, *Acc. Chem. Res.* **1993**, *26*, 593−598.

[38] S. Mecozzi, A. P. West, Jr., D. A. Dougherty, *J. Am. Chem. Soc.* **1996**, *118*, 2307−2308.

[39] J. C. Ma, D. A. Dougherty, *Chem. Rev.* **1997**, *97*, 1303−1324.

[40] G. W. Coates, A. R. Dunn, L. M. Henling, D. A. Dougherty, R. H. Grubbs, *Angew. Chem.* **1997**, *36*, 248−251.

[41] G. W. Coates, A. R. Dunn, L. M. Henling, J. W. Ziller, E. B. Lobkovsky, R. H. Grubbs, *J. Am. Chem. Soc.* **1998**, *120*, 3641−3649.

[42] F. G. Klärner, U. Burkert, M. Kamieth, R. Boese, J. Benet-Buchholz, *Chem. Eur. J.* **1999**, *5*, 1700−1707.

[43] P. Metrangolo, G. Resnati, *Chem. Eur. J.* **2001**, *7*, 2511−2519.

[44] G. W. Gokel, L. J. Barbour, R. Ferdani, J. Hu, *Acc. Chem. Res.* **2002**, *35*, 878−886.

[45] J. Catalán, C. Díaz, F. García-Blanco, *J. Org. Chem.* **2001**, *66*, 5846−5852.

[46] F. G. Bordwell, X. M. Zhang, *Acc. Chem. Res.* **1993**, *26*, 510−517.

[47] Z. Otwinowski, W. Minor "Processing of X-ray Diffraction Data Collected in Oscillation Mode", *276: Macromolecular Crystallography Part A. Methods in Enzymology*, (Eds.: C. W. Carter, Jr., R. M. Sweet), Academic Press, New York, **1997**, pp. 307−326.

[48] *International Tables for Crystallography, vol C: Mathematical, Physical and Chemical Tables*, (Ed.: T. H. Hahn), Kluwer Academic Publishers, Holland, **1992**.

[49] C. L. Perrin, *Mathematics for Chemists*, Wiley-Interscience, New York, **1970**.

[50] J. Chen, A. Cammers-Goodwin, *Tetrahedron Lett.* **2003**, *44*, 1503−1506.

Received May 15, 2003

